J Biomol NMR (2012) 53:113–124
DOI 10.1007/s10858-012-9629-2

ARTICLE

Selective editing of Val and Leu methyl groups in high molecular weight protein NMR

Weidong Hu · Andrew T. Namanja · Steven Wong · Yuan Chen

Received: 15 January 2012 / Accepted: 10 April 2012 / Published online: 25 April 2012

Abstract The development of methyl-TROSY approaches and specific ^{13}C–^{1}H labeling of Ile, Leu and Val methyl groups in highly deuterated proteins has made it possible to study high molecular weight proteins, either alone or in complexes, using solution nuclear magnetic resonance (NMR) spectroscopy. Here we present 2-dimensional (2D) and 3-dimensional (3D) NMR experiments designed to achieve complete separation of the methyl resonances of Val and Leu, labeled using the same precursor, α-ketoisovalerate or acetolactate. The 2D experiment can further select the methyl resonances of Val or Leu based on the C_α or C_β chemical shift values of Val or Leu, respectively. In the 3D spectrum, the methyl cross peaks of Val and Leu residues have opposite signs; thus, not only can the residue types be easily distinguished, but the methyl pairs from the same residue can also be identified. The feasibility of this approach, implemented in both 2D and 3D experiments, has been demonstrated on an 82 kDa protein, malate synthase G. The methods developed in this study will reduce resonance overlaps and also facilitate structure-guided resonance assignments.

Keywords Leucine · Valine · Methyl · Residue-type editing · Malate synthase G

Electronic supplementary material The online version of this article (doi:10.1007/s10858-012-9629-2) contains supplementary material, which is available to authorized users.

W. Hu · A. T. Namanja · S. Wong · Y. Chen (✉)
Departments of Immunology and Molecular Medicine, Beckman Research Institute of City of Hope, Duarte, CA 91010, USA
e-mail: ychen@coh.org

Introduction

It is now possible to study proteins larger than 1 mDa by using the methyl-transverse relaxation optimized spectroscopy (TROSY) NMR approach on U–^{2}H, U–^{13}C-labeled samples with protonated methyl groups (Tugarinov et al. 2003). Some examples of such studies include the determination of the structural basis for signal-sequence recognition by SecA, a 204 kDa ATPase motor of Sec translocase, which was labeled with Ile-[$\delta1$ $^{13}CH_3$], Leu-[$^{13}CH_3$, $^{12}CD_3$], Val-[$^{13}CH_3$, $^{12}CD_3$] and Met-[$^{13}CH_3$] (Gelis et al. 2007). A similar labeling strategy was applied in a series of studies on the 670 kDa 20S core particle (CP) of the proteasome. These studies sought to investigate the dynamics of the CP and its interaction with the 11S activator—a 1.1 mDa complex (Sprangers and Kay 2007); the mechanism of action of a new class of CP proteasome inhibitors (Sprangers et al. 2008); the proteasome gating mechanism (Religa et al. 2010); and the folding, stability and dynamics of a substrate protein in the proteasome antechamber (360 kDa) (Ruschak et al. 2010). More recently, this strategy has been used to investigate the complex of a member of the high mobility group nucleosomal (HMGN) protein family with the nucleosome (230 kDa) to gain new insights into how HMGNs regulate chromatin structure, and the role of phosphorylation in the dissociation of HMGNs from chromatin (Kato et al. 2011). The protonated methyl resonances of Ile ($\delta1$), Val (γ) and Leu (δ) are ideal probes for studies of such macromolecular systems because of their sharp NMR resonances due to rapid rotations about their threefold symmetry axis, as well as their greater intensity afforded by the three equivalent protons. In addition, these methyl-containing residues (Ile, Val, and Leu) are widely distributed throughout the hydrophobic core and the surface of most proteins (Janin

et al. 1988; McCaldon and Argos 1988; Tjong et al. 2007). Furthermore, unlike ^{1}H–^{15}N TROSY (Pervushin et al. 1997), the ^{1}H–^{13}C methyl-TROSY effect that is embedded in the ^{1}H–^{13}C heteronuclear multiple quantum coherence (HMQC) scheme for methyl groups, is independent of magnetic field strengths, and thus an ultra-high magnetic field is not a critical factor for such studies (Tugarinov et al. 2003).

Methyl resonance overlap represents one of the main challenges in NMR studies of high molecular weight proteins, particularly in the absence of an ultra-high magnetic field. Although the selective labeling of protonated methyl groups of Ile can be introduced by a unique precursor, α-ketobutyrate (Gardner and Kay 1997), the protonated methyl pairs of Val and Leu are labeled simultaneously from the same precursor, α-ketoisovalerate (Goto et al. 1999) or acetolactate (Gans et al. 2010). Based on the chemical shift statistics for Val and Leu in proteins deposited in the Biological Magnetic Resonance Data Bank, 95 % of these methyl cross peaks are confined in a spectral area bounded by 18.3–27.7 ppm along the ^{13}C dimension and 0.13–1.35 ppm along the ^{1}H dimension. For a given monomeric polypeptide of 1,000 amino acids, there are typically about 300 methyl cross peaks of Val and Leu in this small region, resulting in severe resonance overlap. To reduce the resonance degeneracy, most studies of high molecular weight complexes have been conducted with labeling of selective subunits of the complexes, or have achieved resonance assignments using the "divide and conquer" approach by assigning isolated domains or subunits first, and then transferring these assignments to intact proteins. Several other methods have been proposed to address the challenge of resonance degeneracy. A new labeling scheme has been introduced in which only pro-S methyl groups of Val and Leu are protonated through the use of 2S [^{1}H, ^{13}C]-labeled acetolactate in the expression media (Gans et al. 2010). This labeling method reduces the number of cross peaks of Val and Leu methyl groups by half, and allows stereospecific assignments for the methyl groups; however, it does not distinguish between the methyl cross peaks of Val and Leu. Two NMR methods, both based on the ^{13}C chemical shift of the carbon directly bonded to the methyl group, were presented previously to obtain residue-type-specific editing of the methyl spectra (Guo and Tugarinov 2010; Van Melckebeke et al. 2004). These methods allowed the complete separation of the methyl resonances of Ala from Thr, but not of Val from Leu, because the carbon chemical shifts between C_β of Val and C_γ of Leu are close to each other.

Residue type editing significantly facilitates site-specific assignments of methyl resonances, which is a bottleneck in NMR studies. Recently, different approaches have been proposed to directly assign methyl resonances without backbone assignments based on known crystal structures. These approaches include comparing the predicted and measured pseudocontact shifts induced by a site-specific paramagnetic label or comparing the predicted and measured chemical shifts and nuclear Overhauser effects (John et al. 2007; Xu et al. 2009). In using these structure-based assignment strategies, information on residue types is necessary to reduce ambiguity. Site-directed mutations have also been used in assignments of methyl resonances (Gelis et al. 2007); however, this approach is extremely tedious and cannot assign overlapped resonances.

In this study, we have developed NMR experiments that allow residue type editing based on the ^{13}C resonances of carbons that are two bonds away from the methyl carbon of Val and Leu. This method has been implemented in both 2-dimensional (2D) and 3-dimensional (3D) experiments. The ^{1}H–^{13}C 2D correlation experiment allows for the clean separation of methyl groups of Leu and Val due to the large chemical shift difference between the C_α of Val and C_β of Leu. In the 2D experiments, Val and Leu methyl cross peaks can be further selectively detected based on their C_α (Val) or C_β (Leu) chemical shift ranges. In the 3D experiment, the Val and Leu cross peaks have opposite signs, allowing straightforward identification of the residue types. In addition, the 3D experiment allows identification of the intra-residue methyl pairs for Val and Leu. The feasibilities of both the 2D and 3D experiments have been demonstrated using an 82 kDa protein, [Ile(δ1-$^{13}CH_3$), Leu($^{13}CH_3$, $^{13}CH_3$), Val($^{13}CH_3$, $^{13}CH_3$)]-U-[^{15}N, ^{13}C, ^{2}H]-malate synthase G (MSG).

Materials and methods

MSG sample preparation

The pET28+ expression plasmid for the *E. coli* protein MSG (82 kDa), a generous gift from Dr. Vitali Tugarinov, was transformed into the *E. coli* BL21(DE3) codon plus strain. His-tagged MSG protein for labeling valine/leucine methyl groups was expressed and purified using the modified protocols by Marley et al. (2001) and Tugarinov et al. (2002). Briefly, *E. coli* cells containing the MSG expression plasmid were grown (37 °C, in 1 L LB medium) to an OD_{600} of ~0.5, washed with 1 L M9 medium that lacked NMR isotopes and then re-suspended in 250 mL M9 medium containing 0.25 g $^{15}NH_4Cl$, 1 g [$^{13}C_6$, D_7]-glucose, 100 % D_2O, and the sodium salts of [$^{13}C_4$, 3,3-D_2]-alpha-ketobutyric acid (98 % ^{13}C, 98 % ^{2}H) (35 mg) and [$^{13}C_5$, 3-D_1]-alpha-ketoisovaleric acid (98 % ^{13}C, 98 % ^{2}H) (65 mg). All NMR isotopes were obtained from Cambridge Isotopes Laboratories (Cambridge, MA). After incubation to exhaust the remaining LB metabolites (1 h, 37 °C), the

M9 culture was treated with 1 mM Isopropyl β-D-1-thio-galactopyranoside (IPTG) at 30 °C to induce expression of [U-^{15}N, U-^{13}C, Ile(δ1-$^{13}CH_3$), Leu($^{13}CH_3$, $^{13}CH_3$), Val($^{13}CH_3$, $^{13}CH_3$)]-labeled MSG. The cells were harvested after 13 h and lysed using the Bugbuster protein extraction kit (Novagen). Purification was performed by affinity chromatography on Ni–NTA agarose (Qiagen). The final NMR samples (0.3–0.6 mM) were exchanged into 20 mM sodium phosphate buffer, pH 7.1, containing 20 mM $MgCl_2$, 0.03 % NaN_3, 5 mM DTT-D_{10}, and 10 % D_2O.

NMR experiments

All NMR experiments were carried out at 37 °C on a Bruker Avance 600 MHz spectrometer equipped with a cryogenic and shielded z-axis triple-resonance probe. The 2D ^{1}H–^{13}C constant time HMQC experiment was acquired with 28 ms as the constant time, 2,048 and 112 complex points for the ^{1}H and ^{13}C dimensions, respectively, and 107 and 14.8 ms as acquisition times for the ^{1}H and ^{13}C dimensions, respectively. The experiment took 35 min using 16 scans and a recycle delay of 1 s. All other 2D ^{1}H–^{13}C correlation experiments used the same parameters, with the following differences: the number of scans was 80 and the recycle delay was 1.2 s; thus the experiment time was 3 h, 36 min. The constant time was set to 28.5 ms for 2D V/L-CT-H_mC_m and 29.2 ms for 2D L-CT-H_mC_m. For the 3D VL-CT-H_mC_mC experiment, the data was acquired with 28 ms constant time; 78, 74, and 2,048 complex points for the C, C_m and H_m dimensions, respectively; and 9.9, 9.8, and 107 ms acquisition times for the C, C_m and H_m dimensions, respectively. The experiment time was 37 h using 16 scans and a 1.2 s recycle delay.

All NMR data were processed using the NMRPipe/NMRDraw software package (Delaglio et al. 1995). The points in the methyl carbon dimensions of all data sets were doubled using the mirror-image linear prediction method (Zhu and Bax 1990) before apodization and Fourier transformation. The spectra were analyzed using NMRView software (Johnson and Blevins 1994). We used C_α chemical shifts of Val and C_β chemical shifts of Leu in MSG of the previous assignments (Tugarinov et al. 2002). The ^{1}H and ^{13}C chemical shifts of methyl groups and the stereo-specific assignments of Val and Leu in MSG were from previous studies (Gans et al. 2010; Tugarinov and Kay 2003, 2004b).

Results

Experimental design

Figure 1 shows the pulse sequences used to separate the methyl resonances of Val and Leu in perdeuterated and ^{13}C-labeled protein samples. The approach relies on the large chemical shift difference between the C_α of Val and the C_β of Leu and Val and the C_γ of Leu, as well as on the use of selective inversion pulse and $^1J_{C-C}$ scalar coupling. Figure 1A shows the pulse sequence for 2D constant time (CT) experiments for the detection of either Val or Leu methyl resonances (2D V/L-CT-H_mC_m, where H_m and C_m refer to ^{1}H and ^{13}C of the methyl groups, respectively). The same experiment can also be used to detect a sub-set of methyl groups from Val or Leu. The pulse sequence shown in Fig. 1B is optimized for the detection of all Leu methyl resonances (2D L-CT-H_mC_m), and is also a constant time ^{1}H–^{13}C correlation experiment. A 3D experiment (Fig. 1C) was designed to detect Val and Leu simultaneously (VL-CT-H_mC_mC) and correlates C_β of Val or C_γ of Leu with chemical shifts of C_m and H_m. This pulse scheme generates 3D spectrum where Val and Leu cross peaks exhibit opposite signs. Because the 2D and 3D experiments were developed based on the same approach, we will focus our discussion on the sequence shown in Fig. 1A.

The magnetization of the three equivalent methyl protons (H) is first transferred to the methyl carbon (C_m) through the INEPT step and ends at point "a" (Fig. 1A) as the term $2H_zC_y^m$. From point "a" to "b," the magnetization is transferred from the methyl carbon to C_β of Val or C_γ of Leu, and ends as $4H_zC_z^mC_x^\beta$ for Val or $4H_zC_z^mC_x^\gamma$ for Leu. In the constant time period ($2T_C = 28.5$ ms, $1/^1J_{C-C}$) starting at point "b," the $^1J_{C-C}$ scalar coupling between C_β and C_α of Val is used to separate the methyl groups of Val from those of Leu. During the constant time $2T_C$ period, two selective inversion I-BURP pulses (Geen and Freeman 1991) are applied at points $T_C/2$ and $3T_C/2$. The I-BURP pulses are both alternatively applied at 62 and −62 ppm for two consecutive scans. If the two I-BURP pulses are on-resonance at C_α of Val (62 ppm), the scalar coupling between C_β and C_α is refocused and the term $4H_zC_z^mC_x^\beta$ is not amplitude modulated. Note that the coefficient $\cos^2(2T_C * \pi * J_{c_\beta - c_m})$ of the term $4H_zC_z^mC_x^\beta$, due to the scalar coupling between C_β and the methyl carbons during the constant time period, is not affected by either on- or off-resonance I-BURP pulses, and will not be further discussed. If the two I-BURP pulses are on −62 ppm, the scalar coupling of C_β and C_α results in an extra coefficient, $\cos(2T_C * \pi * J_{c_\beta - c_\alpha})$, for the term $4H_zC_z^mC_x^\beta$. This reverses the sign of $4H_zC_z^mC_x^\beta$ because $2T_C$ is set to $1/^1J_{C-C}$. In this way, the sign of Val resonances is reversed every other scan due to the I-BURP irradiating on and off C_α resonance every other scan. The 2 ms I-BURP pulse covers approximately 13 ppm in the ^{13}C dimension on a 600 MHz NMR instrument; thus, the sign and amplitude of the Leu term $4H_zC_z^mC_x^\gamma$ are not affected by on- and off-resonance I-BURP pulses. After the constant time period, the methyl

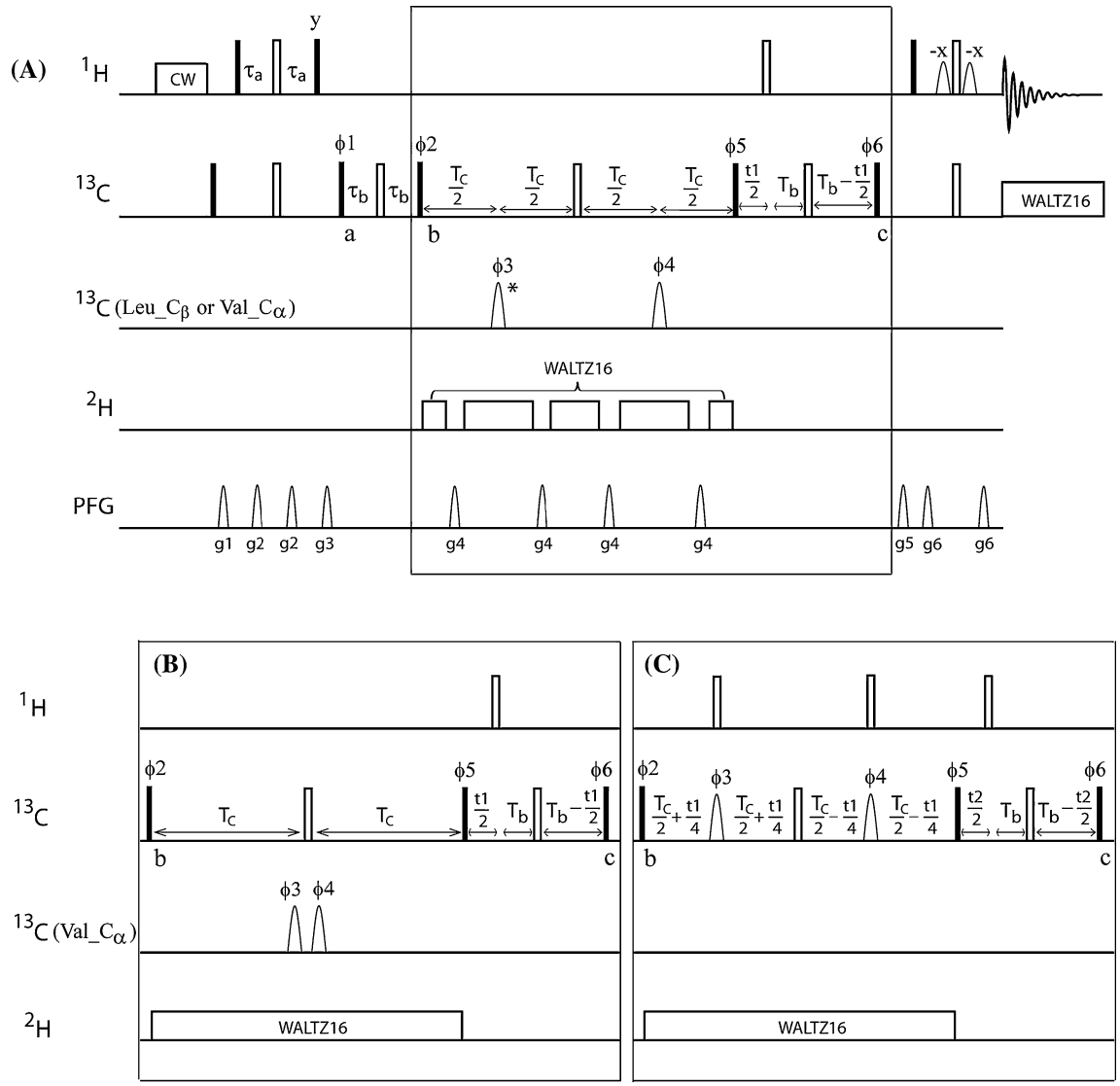

Fig. 1 Pulse sequences for separating the methyl groups of Val and Leu in [L($^{13}CH_3$, $^{13}CH_3$), V($^{13}CH_3$,$^{13}CH_3$)]-U-[^{15}N, ^{13}C, ^{2}H]-protein samples. **A** The 2D V/L-CT-H_mC_m pulse scheme for detecting the methyl spectrum of Val or Leu separately. This scheme also allows detection of a subset of methyl groups based on the C_α chemical shift of Val or C_β chemical shift of Leu. All radio frequency pulses are applied along the x-axis unless otherwise indicated. The hard 90° and 180° pulses on ^{1}H and ^{13}C are represented using *filled* and *open rectangular bars*, respectively. The field strengths for ^{1}H pre-saturation, ^{13}C WALTZ-16 (Shaka et al. 1983), and ^{2}H WALTZ-16 decoupling are 12 Hz, 3.1 kHz and 1 kHz, respectively. The ^{13}C carrier is put at 19.5 ppm first, and then switched to 43.5 ppm before the ^{13}C pulse with phase $\phi1$ at point "a." Delays are $\tau_a = 1.8$ ms; $\tau_b = 7$ ms; $T_C = 14.25$ ms and $T_b = 7.5$ ms. The phase cycling parameters are: $\phi1 = x, -x$; $\phi2 = 2(y), 2(-y)$; $\phi3 = \phi4 = 2(x), 2(-x), 2(y), 2(-y)$; $\phi5 = 4(y), 4(-y)$; $\phi6 = 8(x), 8(-x)$; rec = 8(x), 8(−x). Quadrature detection in t_1 is achieved by incrementing $\phi6$ using the STATES-TPPI scheme (Marion et al. 1989). The pulsed field gradients, g1 to g6, are applied along the z-axis with strengths (G/cm)/duration (ms) of: g1 = 11/1.0, g2 = 5.5/1.0, g3 = 16.6/1.0, g4 = 22/1.0, g5 = 39.5/0.5, g6 = 39.5/0.5. The durations of the selective 180° I-BURP pulses (Geen and Freeman 1991) with $\phi3$ and $\phi4$ are 2 ms for detecting all methyl groups of Val or Leu, and 12 ms for detecting a subset of methyl groups of Val or Leu. The I-BURP pulses are applied at 62 and −62 ppm alternately for two consecutive scans to detect all methyl groups of Val or Leu. To detect all methyl groups of Leu, the receiver phase cycling is changed to 4(x, −x), 4(−x, x), and the I-BURP pulse labeled with asterisk ($\phi3$) is moved leftward 1.65 ms (see "Discussion" in text). **B** The 2D L-CT-H_mC_m pulse scheme optimized for detection of all methyl groups of Leu residues. Most of the parameters are the same as described in **A**, with the following changes: T_C is set to 14.6 ms and the two 180° I-BURP pulses ($\phi3$ and $\phi4$) are replaced with two 90° E-BURP pulses applied at 62 ppm with a duration of 1.8 ms. The phase cycling parameters are $\phi1 = x, -x$; $\phi2 = 2(y), 2(-y)$; $\phi3 = 2(y), 2(-y)$; $\phi4 = 4(x), 4(-x)$; $\phi5 = 4(y), 4(-y)$; $\phi6 = 8(x), 8(-x)$; rec = 4(x, −x), 4(−x, x). The STATES-TPPI scheme is applied on $\phi6$ for quadrature detection in t_1. (C) The 3D VL-CT-H_mC_mC pulse scheme used to correlate the Val and Leu methyl groups to the directly attached carbon. Most of the parameters are the same as described in **A**, with the following differences. T_C is set to 14 ms. The phase cycling parameters are: $\phi1 = x, -x$; $\phi2 = 2(y), 2(-y)$; $\phi3 = \phi4 = 2(x), 2(-x), 2(y), 2(-y)$; $\phi5 = 4(y), 4(-y)$; $\phi6 = 8(x), 8(-x)$; rec = 4(x, −x), 4(−x, x). The quadrature detection uses the STATES-TPPI scheme in t_1 on phase $\phi1$ and $\phi2$, and in t_2 on $\phi6$. The selective pulses with $\phi3$ and $\phi4$ are I-BURP on resonance applied at 62 ppm with a duration of 2 ms

carbon chemical shifts are labeled and the antiphase terms of C_β of Val and C_γ of Leu are refocused in the constant time $2T_b$. Finally, the magnetization is transferred back to the methyl proton and detected. Because the signs of the Val cross peaks are reversed every other scan in conjunction with the on- and off-resonance I-BURP pulses, while the Leu peaks are not affected by the I-BURP pulses, the methyl peaks of Val or Leu residues are easily selected by manipulating the receiver phase cycling. Although the sequence in Fig. 1A is designed to detect Val cross peaks, Leu cross peaks can be detected if the receiver phase is changed to 4(x, −x), 4(−x, x). Alternatively, the sequence can be implemented in an interleaved manner, and store the data acquired from both on and off-resonance separately. Similar to Leu, in samples labeled with Ile-(δ1-$^{13}CH_3$), the coherence of Ile is not affected by the I-BURP pulses, and the Ile δ1-methyl groups are detected together with the Leu methyl groups and are not in the Val methyl spectrum. The sign of Ile δ1-methyl groups is opposite to that of the Leu methyl groups, because only one methyl is attached at the $C_{\gamma 1}$ position of Ile. The δ1-methyl cross peaks of Ile will not be shown in the following discussions, because they are well separated from Leu and Val methyl resonances. An alternative design for these types of experiments is to take full advantage of the methyl-TROSY effect by keeping the methyl ^1H–^{13}C magnetization in the multiple quantum (MQ) state during the $2\tau_b$ and $2T_b$ periods instead of the single quantum state. This strategy was reported in the 4D HMCBCACO experiment (Sheppard et al. 2009). The pulse sequence with this strategy implemented is shown in Supplemental Figure S1. This approach works better on the sample with ($^{13}CH_3$, $^{12}CD_3$)-labeling scheme for two methyl groups in Leu and Val (Tugarinov and Kay 2004a).

Although Leu methyl groups can be detected using the pulse scheme in Fig. 1A, as described above, inspection of the Leu spectrum showed weak leakage from a few of the strongest Val peaks (circled region, Fig. 5A). The more clean cancelation of the Leu signals is due to both on and off resonance irradiation on the Val C_α not affecting the Leu signals. However, the on and off resonance irradiation on the Val C_α has differential effects on Val signals due to non-uniform J coupling constants and differential relaxation rates, leading to imperfect subtraction of Val signals that are visible for the sharpest resonances. A similar phenomenon has been reported in experiments using $^1J_{C-C}$ to separate Pro-R and Pro-S methyl groups of Val and Leu (Hu and Zuiderweg 1996), and to selectively detect methyl groups (Van Melckebeke et al. 2004). The leakage cannot be eliminated completely by optimizing the constant time duration. Therefore, the position of the first I-BURP shape pulse (Fig. 1A, labeled with asterisk) was moved gradually leftwards from the middle point of the first T_C period. The optimal delay for MSG was found to be 1.65 ms for the best suppression of leakage, when the strongest Val resonances were suppressed to the noise level. However, this delay appears to be protein-dependent when optimization was conducted for a smaller protein. The protein-dependent position adjustment of the selective pulse indicates that the leakage is more likely to be due to differential relaxation of inphase and antiphase magnetization than incomplete enrichment of the precursor (98 % ^{13}C enriched) and non-uniform J-coupling. Since Leu spectrum needs special optimization using sequence Fig. 1A as discussed above, we decided to use a different design to obtain a clean Leu spectrum.

To acquire a cleaner Leu methyl spectrum without optimizing the delay, a different approach was designed (Fig. 1B). The key feature is the change of the two 180° I-BURP pulses to 90° E-BURP pulses that cover the C_α region of Val. The E-BURP positioned at the end of the T_C period ($1/2^1J_{C-C}$) is used to transfer the anti-phase term between C_β and C_α ($C_y^\beta C_z^\alpha$) to multiple-quantum coherence $C_y^\beta C_x^\alpha$, which cannot be transferred back to an NMR-detectable term during the subsequent steps of the pulse sequence. The second E-BURP, which has a 90° phase shift from the first E-BURP and is placed after the 180° hard pulse, is used to compensate for the Bloch-Siegert shift and to further convert the residual term $C_y^\beta C_z^\alpha$ into an undetectable term $C_y^\beta C_x^\alpha$. Similarly, the Val magnetization is purged again by transferring to an undetectable term at the end of the second T_C period by the hard 90° ($\phi 5$) pulse while the Leu magnetization is converted to $4H_zC_x^mC_z^\gamma$ for final detection. By purging the Val magnetization twice during the two T_C ($1/2^1J_{C-C}$) periods, the sequence shown in Fig. 1B produced a clean Leu methyl spectrum. The δ1-methyl groups of Ile were also detected in this spectrum, but their cross peaks had the opposite sign from those of Leu.

The 2D V/L-CT-H_mC_m pulse scheme was extended into a 3D experiment (Fig. 1C) by adding a ^{13}C dimension to detect C_β of Val and C_γ of Leu in the constant time period $2T_C$ ($1/^1J_{C-C}$) concomitantly with sign discrimination of Val and Leu cross peaks. The sign discrimination is achieved by applying two on-resonance I-BURP pulses on C_α of Val in the middle of two T_C periods. Because the scalar coupling between C_α and C_β of Val is refocused by the two I-BURP pulses, the sign of Val coherence is not changed at the end of the $2T_C$ period. For Leu, the scalar coupling between C_γ and C_β results in a coefficient $\cos(2T_C * \pi * J_{c_\gamma - c_\beta})$, which reverses the sign of the Leu signal at the end of the constant time period ($1/^1J_{C-C}$). After the constant time period, the methyl carbon is evolved in

the $2T_b$ time period, and finally the magnetization is transferred back to the methyl ^{1}H for detection.

Separation of the methyl groups of Val and Leu

We tested the pulse sequences on several proteins with sizes ranging from 11 to 82 kDa, including the 82 kDa MSG protein (Fig. 2). The acquisition times for both the ^{1}H and ^{13}C dimensions for all of the spectra shown in Fig. 2 were the same to ensure an unbiased comparison. The spectrum acquired using the CT-HMQC sequence (Marino et al. 1997) is shown in Fig. 2A. Figure 2B shows the superimposition of the ^{1}H–^{13}C methyl correlation spectra of Val (blue) and Leu (red) acquired using the pulse sequences shown in Fig. 1A, B, respectively. The majority of the Val and Leu methyl resonances were located in the same region of the NMR spectra; therefore, it was impossible to distinguish the 46 Val methyl resonances from the 70 Leu methyl resonances of the 82 kDa MSG based only on their chemical shifts (Fig. 2A). However, the experiments presented herein can easily assign the residue-type for these methyl resonances and reduce overlap (Fig. 2B). To further illustrate the results, we chose three areas of the 2D CT-HMQC (indicated by arrows in Fig. 2A) for additional analysis. There are two overlapped methyl cross peaks of V259$_{\gamma 1}$ and L54$_{\delta 2}$ at position 1 (indicated by an arrow) in the 2D CT-HMQC spectrum (Fig. 2A, B), but these two cross peaks are completely resolved in the selective spectra for Leu (Fig. 2C) and for Val (Fig. 2D). Similarly, the cross peaks of L454$_{\delta 2}$ and V20$_{\gamma 1}$ are exactly superimposed at position 2 in the 2D CT-HMQC spectrum (Fig. 2A, B), yet are separated in the selective spectra (Fig. 2C, D). At position 3, three Val cross peaks (V535$_{\gamma 1}$, V600$_{\gamma 2}$ and V43$_{\gamma 2}$) became well resolved in the selective Val spectra (Fig. 2D) after separation from the overlapping Leu cross peaks (Fig. 2C).

The cross peaks in the 3D spectrum correlate H_m-C_m-C_β for Val and H_m-C_m-C_γ for Leu, but with the sign of the Val cross peaks was opposite from that of Leu (Fig. 3). The 3D spectrum significantly resolved resonance overlaps (Fig. 3A, B). Figure 3A shows an expanded region of the superimposed 2D Val- (blue) and Leu-selected (red) spectra (Fig. 2B) that contained overlapped resonances. Figure 3B shows the 2D plane that correlates C_m with C_β

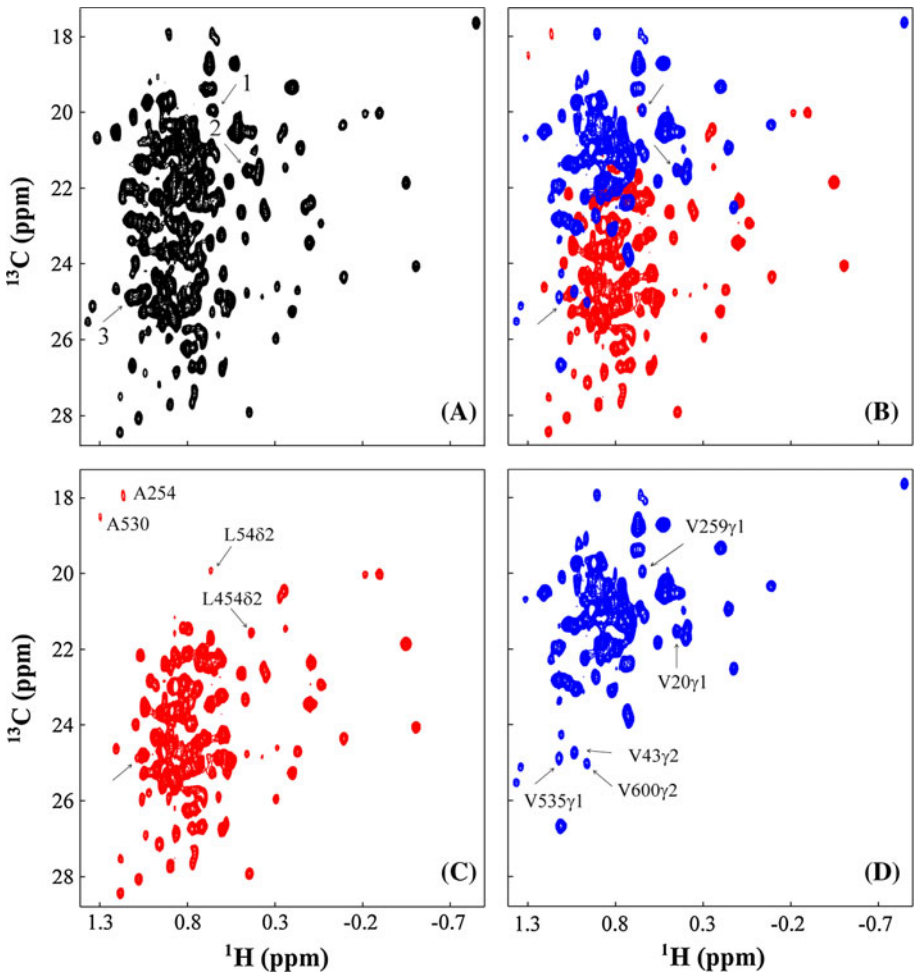

Fig. 2 Leu and Val-selective spectra acquired on [I(δ1-^{13}CH$_3$), L(^{13}CH$_3$, ^{13}CH$_3$), V(^{13}CH$_3$, ^{13}CH$_3$)]-U-[^{15}N, ^{13}C, ^{2}H]-MSG at 37 °C. **A** The methyl region of Val and Leu acquired using CT-HMQC for comparison. **B** The overlay of Leu- (*red*) and Val-selective (*blue*) methyl spectra acquired using the 2D L-CT-H_mC_m and the 2D V/L-CT-H_mC_m pulse schemes, respectively. Three overlapped positions are indicated with *numbered arrows* in both **A** and **B**. The two spectra are shown separately in (**C**, Leu) and (**D**, Val). The assignments at the three positions are indicated according to previously reported assignment (Gans et al. 2010; Tugarinov and Kay 2004b) and the overlapped Val and Leu resonances are resolved in the selective spectra **C** and **D**

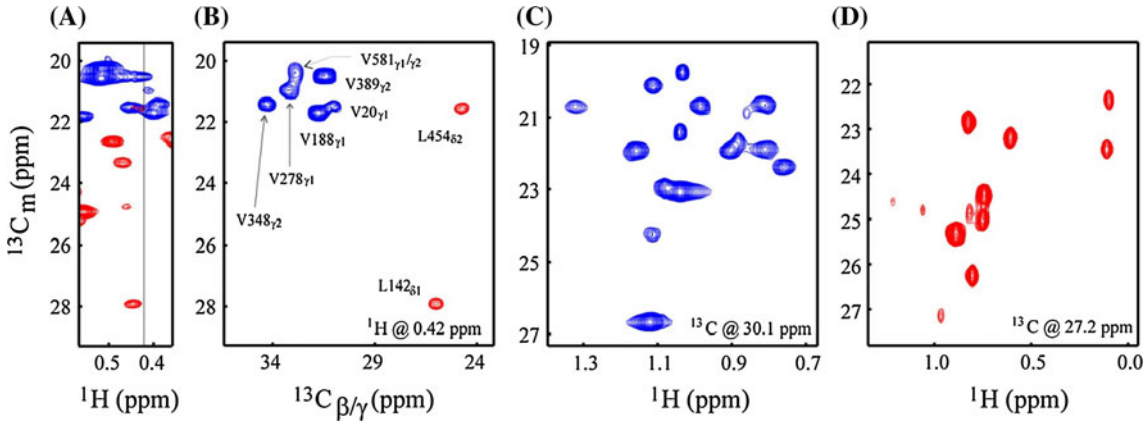

Fig. 3 Representative 2D planes of the 3D spectrum for MSG acquired using the 3D VL-CT-H_mC_mC experiment at 37 °C. Val (*blue*) and Leu (*red*) residues were distinguished based on their opposite signs. **A** Strip of the overlay of 2D Leu- and Val-selective spectra from Fig. 2B. **B** The 2D ^{13}C–^{13}C plane of the 3D spectrum with the ^1H anchored at 0.42 ppm, indicated by the vertical line in **A**. **C** and **D** Representative 2D ^{13}C–^1H methyl correlation slices of the 3D data for **C** Val with the ^{13}C (C_β) dimension at 30.1 ppm and **D** Leu with the ^{13}C (C_γ) dimension at 27.2 ppm

of Val and C_γ of Leu anchored at 0.42 ppm of the ^1H dimension, in which the overlapped resonances of L454$_{\delta2}$ and V20$_{\gamma1}$ (Figs. 2B, 3A) are well resolved and have opposite signs. In addition, the six Val cross peaks with ^1H_m chemical shift close to 0.42 ppm are better separated (labeled in Fig. 3B). The 2D H_m-C_m correlation planes of the 3D spectrum (Fig. 3C, D) significantly resolve the crowdedness of the 2D HMQC spectrum by adding a third dimension. For example, all methyl cross peaks observed in the 2D $^{13}C_m$–^1H_m plane, anchored at 30.1 ppm in the t_1-dimension, showed the sign that indicated Val resonances (Fig. 3C), therefore these peaks are identified to belong to the Val residue-type. This 2D plane (Fig. 3C) shows much better resolved resonances than the corresponding region of the 2D Val-selected spectrum (Fig. 2D). Similarly, another 2D plane anchored at 27.2 ppm shows cross peaks that all have the sign of Leu residues (Fig. 3D). Again, this 2D plane shows much better resolved resonances than the corresponding region of the 2D Leu-selective spectrum (Fig. 2C). It is worth noting that through the correlation of a given methyl group with the attached carbon, the 3D experiment can also be used to identify the intra-methyl pairs of Val and Leu.

Selective detection of a sub-set of Val or Leu methyl groups

To further resolve the overlapped peaks in the spectra of Leu or Val, we applied a 12 ms I-BURP pulse in the sequence shown in Fig. 1A to selectively inverse a small band of C_β of Leu or C_α of Val. In this way, only a limited number of methyl groups (pairs) corresponding to a user-defined range of C_β (Leu) or C_α (Val) were detected. We demonstrated the utility of this method for both Val (Fig. 4) and Leu (Fig. 5) of MSG. In order to detect most of the Val resonances, six sub-spectra were acquired with I-BURP irradiation frequencies at 58, 60.4, 62.6, 63.4, 65.6 and 68.1 ppm. Figure 4A shows the spectrum of all Val methyl groups acquired with a 2 ms I-BURP pulse applied at 62 ppm. Representative Val sub-spectra corresponding to a 12 ms I-BURP applied at 58, 62.6 and 65.6 ppm are shown in Fig. 4B–D, respectively. In comparison to Fig. 4A, there are considerably fewer cross peaks in the three sub-spectra. For example, the two overlapped peaks of V386$_{\gamma1}$ and V193$_{\gamma1}$ (Fig. 4A, boxed region and inset) are separated in the sub-spectra (Fig. 4B, C). The C_α chemical shifts of V386 and V193 were 59.9 and 61.1 ppm, respectively. Similarly, V24$_{\gamma1}$ (C_α at 64.4 ppm) overlaps with V581$_{\gamma1}$ (C_α at 59.2 ppm) in the Val-selective spectrum (Fig. 4A), but becomes completely resolved in the sub-spectra (Fig. 4C, D, insets). Also, the overlapped V389$_{\gamma2}$ (C_α at 61.6 ppm) and V464$_{\gamma1}$ (C_α at 58.8 ppm) appear in different sub-spectra (Fig. 4C, B, respectively), and thus are well resolved. Similarly, the partially overlapped V259$_{\gamma2}$ (C_α at 61.2 ppm) and V43$_{\gamma1}$ (C_α at 67.3 ppm) appear in different sub-spectra (Fig. 4C, D, respectively).

The same approach was also applied to selectively detect Leu methyl resonances. A 12 ms I-BURP pulse at C_β of Leu produced sub-spectra of Leu methyl resonances (Fig. 5). To cover all methyl cross peaks in the Leu sub-spectra, a 12 ms I-BURP pulse was applied at six Leu C_β chemical shifts of 37.4, 39.5, 41.5, 42.3, 44.4 and 46.5 ppm in six different sub-spectra. Overlapped Leu methyl resonances (Fig. 5A, boxed region and inset) are further resolved in the sub-spectra (Fig. 5B–D). Only one of the six cross peaks in the boxed region of Fig. 5A, L514$_{\delta2}$ (C_β at 38.1 ppm), is detected in the sub-spectrum obtained with the 37.4 ppm I-BURP (Fig. 5B). This peak is well

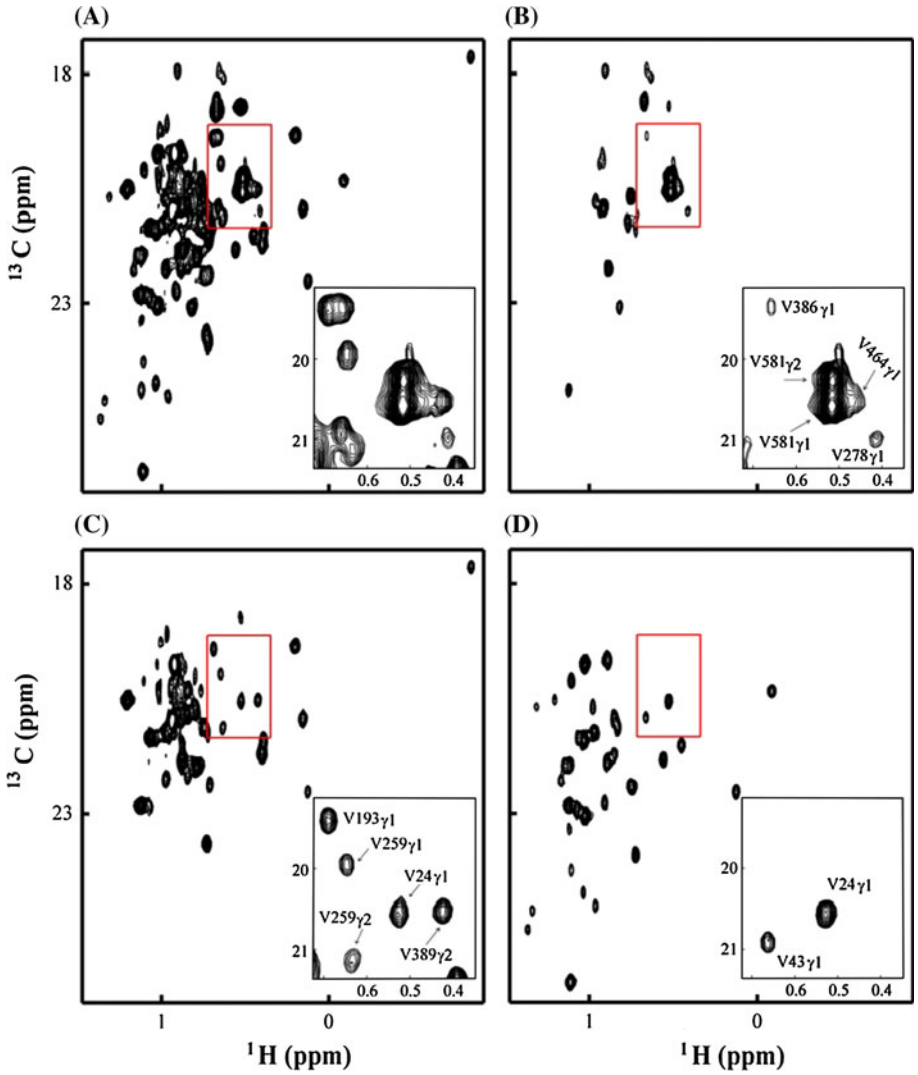

Fig. 4 Full and representative sub-spectra of Val methyl cross peaks acquired using 2D V/L-CT-H_mC_m. **A** Full spectrum of Val methyl resonances. **B–D** Sub-spectra acquired with a 12 ms I-BURP pulse applied at **B** 58, **C** 62.6 and **D** 65.6 ppm. The overlapped cross peaks in the outlined region in **A** are resolved in the sub-spectra shown in **B–D** and their assignments are indicated. All *insets* are enlargements of the respective regions outlined in *red*

separated from L210$_{\delta 2}$ (C_β at 42.1), which is detected in a sub-spectrum acquired with the I-BURP at 42.3 ppm. We noticed that there is weak leakage from Val 98γ1/2 as labeled in Fig. 5B. The only leakage observed is caused by the small separation between the radiation frequency of I-BURP, at 37.4 ppm, and that of Val 98 C_β, which is at 34.7 ppm. Although the 12 ms I-Burp pulse is very selective, it still disturbs the magnetization of C_β of Val98. The perturbation makes the cancellation of magnetization between on and off I-BURP pulses not perfect for Val98. The C_β chemical shift of V98 is the largest among all the Val residues in MSG. Since the 37.4 ppm is the smallest value used in all six subspectra of Leu, and there are not many cross peaks located in this subspectrum, the small leakage can be easily identified by comparison with Fig. 5A. Although C_δ and C_γ of some Leu residues may potentially have strong coupling interactions, we did not observe line shape distortion among all the Leu sub-spectra, which is in agreement with what was reported before (Vuister and Bax 1992). In the sub-spectra obtained with an I-BURP pulse at 39.5 ppm (Fig. 5C), L514$_{\delta 2}$ is already resolved and labeled (Fig. 5B), and L699$_{\delta 2}$ (C_β at 39.7 ppm) is resolved from the overlap with L210$_{\delta 2}$ (C_β at 42.1 ppm) and L10$_{\delta 2}$ (C_β at 42.9 ppm). On the other hand, the overlap between L413$_{\delta 2}$ (C_β at 40.3 ppm) and L30$_{\delta 2}$ (C_β at 40.8 ppm) is not resolved because of their similar C_β chemical shifts. Because many Leu residues have C_β chemical shifts close to 39.5 ppm, there are more cross peaks in Fig. 5C (I-BURP at 39.5 ppm) than the other sub-spectra. Further reduction of peaks can be achieved by applying a longer shape pulse (essentially by using up all of the constant time duration), adjusting the I-BURP pulse position, or using a different shape pulse, such as the I-SNOB (Kupce et al. 1995), which offers a narrower inversion profile for a given pulse duration. The spectrum in Fig. 5D was acquired with the I-BURP pulse at 44.4 ppm. Again, fewer Leu cross peaks are detected, and only one peak, L10$_{\delta 2}$ (C_β at 42.9 ppm), remains in the

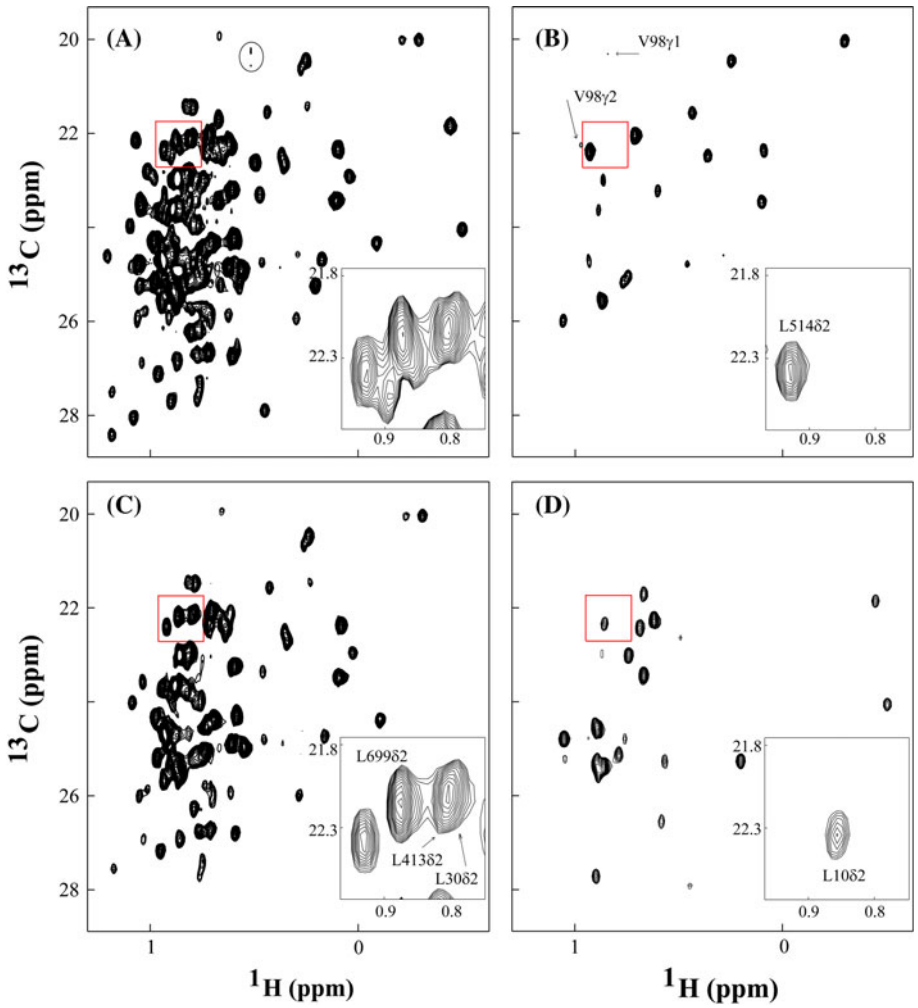

Fig. 5 Full and sub-spectra of Leu methyl cross peaks acquired using 2D V/L-CT-H_mC_m. **A** Full spectrum of Leu methyl resonances. The *circled* region shows weak leakage from the strongest Val resonance (V581, see Fig. 4A) that is completely suppressed by the pulse scheme 2D L-CT-H_mC_m (Fig. 1B), as shown in Fig. 2C. **B**–**D** Sub-spectra acquired with a 12 ms I-BURP pulse applied at **B** 37.4, **C** 39.5 and **D** 44.4 ppm. The overlapped cross peaks in the outlined region in **A** are mostly resolved in the different sub-spectra shown in **B**–**D** and their assignments are indicated. All *insets* are enlargements of the respective regions outlined in *red*

boxed region. In summary, we have shown that resonance overlap of both Val and Leu methyl cross peaks in proteins can be largely resolved in sub-spectra.

Correlation of methyl cross peaks with chemical shifts of Val C_α and Leu C_β

Because the 2D experiment allows selective detection of the methyl groups of Val and Leu based on their corresponding C_α and C_β chemical shift values, respectively, we investigated how to correlate the methyl cross peaks with the chemical shifts of their C_α for Val or C_β for Leu. We compared the peak intensity from two spectra, the sub and full spectra acquired using 12 and 2 ms I-BURP pulses, respectively. In theory, a peak intensity ratio of 1 between the sub and full spectra reflects the complete inversion of the C_α (Val) or C_β (Leu) resonances in the sub-spectra, and a peak intensity ratio less than 1 reflects incomplete inversion in the sub-spectra due to C_α (Val) or C_β (Leu) resonances at the border of the I-BURP inversion profile (Supplemental Figure S2A). The black curve shown in the Supplemental Figure S2A is a 2 ms I-BURP inversion profile used for acquiring the full Val or Leu methyl spectrum, and the red curve is a 12 ms I-BURP inversion profile used for acquiring the sub-spectra of Val or Leu. The complete inversion coverage of the 12 ms I-BURP is 334 Hz, which is about ±1.1 ppm from the irradiation frequency for ^{13}C on a 600 MHz instrument. Therefore, if the peak intensity ratio between the sub and full spectra is approximately 1, the C_α (Val) or C_β (Leu) chemical shifts associated with that peak should be within approximately 1.1 ppm of the irradiation frequency of a 12 ms I-BURP pulse in the sub-spectrum. If the intensity ratio of a peak is significantly less than 1, the C_α (Val) or C_β (Leu) chemical shifts associated with that peak would be at the border of the I-BURP inversion profile, correlating to a narrower chemical shift range.

We demonstrated this approach for MSG. To facilitate the analysis, the peak intensity ratio between the sub and full spectra was normalized by defining the maximum peak intensity ratio as 1.0 in each sub-spectrum. For clarity, the normalized peak intensity ratios of resolved peaks from the

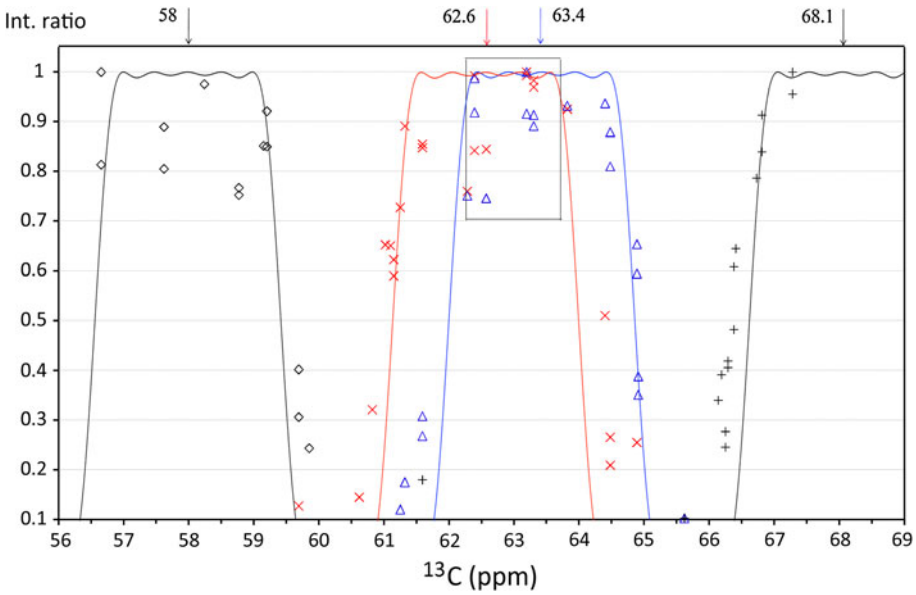

Fig. 6 Methyl peak intensity ratio between the sub and full spectra of Val versus the chemical shift of C_α of Val along with the simulated 12 ms I-BURP inversion profiles. The C_α chemical shifts were identified in a previous report (Tugarinov et al. 2002). The peak intensity ratio was normalized for each sub-spectra by defining the largest ratio within each sub spectra as 1.0. The intensity ratios are color coded according to the *arrows* at the top of the figure that correspond to the I-BURP irradiation frequencies of the different sub-spectra. The peaks indicated by *diamond*, *times*, *triangle*, and *plus sign* are from sub-spectra acquired with I-BURP pulses applied at 58, 62.6, 63.4 and 68.1 ppm, respectively for Val. The *outlined box* in the figure covers the chemical shift range 63 ± 0.7 ppm

four out of six sub-spectra of Val are plotted versus the published C_α (Val) chemical shifts indicated at the bottom horizontal axis of the panels (Tugarinov et al. 2002) in Fig. 6. In the figure, the peak intensity ratios from four sub-spectra are labeled according to their corresponding I-BURP irradiation frequencies as indicated by arrows at the top horizontal axis. Overall, the distribution of peak intensities from the same sub-spectrum outlined a shape similar to the simulated inversion profile curves of a 12 ms I-BURP pulse. For 46 Val residues, there are 55 resolved methyl resonances. Considering uncertainties in intensity estimation, we analyzed peak intensity ratios of 0.7 and larger. Theoretically, 70 % inversion covers 404 Hz, which is about ±1.4 ppm from the irradiation frequency for ^{13}C on a 600 MHz instrument. Some of these methyl cross peaks have intensity ratios above 0.7 in two adjacent sub-spectra; thus, there are a total of 77 peaks with intensity ratios larger than 0.7 from all six sub-spectra. All 77 peaks are within ±1.4 ppm of the irradiation frequency. This result suggests that correlating an intensity ratio larger than 0.7 with the C_α chemical shifts within ±1.4 ppm of a 12 ms I-BURP irradiation frequency is a reliable method. Importantly, comparison of sub-spectra obtained with I-BURP irradiation frequencies near each other allows the prediction of C_α chemical shifts more precisely. For example, the overlapped full inversion region from two sub-spectra acquired by two 12 ms I-BURP pulses positioned 0.8 ppm apart was 204 Hz instead of 334 Hz (Supplemental Figure S2B). This approach was tested by acquiring two sub-spectra, with I-BURP irradiation frequencies at 63.0–0.4 ppm and 63.0 + 0.4 ppm, respectively. The C_α corresponding to the peaks with intensity ratios larger than 0.7 were located within the range of 63.0 ± 0.7 ppm (boxed in Fig. 6).

There are 107 resolved methyl peaks in the six sub-spectra for Leu residues, with intensity ratios greater than 0.7, including some resonances that were counted twice due to appearance in two adjacent sub-spectra. Similar to the analysis for the Val residues, 93 peaks are associated with C_β chemical shifts within ±1.4 ppm of the irradiation frequency of a 12 ms I-BURP pulse. However, 4 peaks have intensity ratios greater than 0.7 but are outside of the ±1.4 ppm range, and 18 peaks have intensity ratios less than 0.7 but are within 1.4 ppm of the irradiation frequency. The less reliability at predicting Leu C_β resonances is due to the larger uncertainty in the intensity estimation (20 % error) that may arise from differential degrees of freedom among the elongated side chains of Leu compared to Val.

Discussion

We have presented new methods to obtain clean separation of Leu and Val methyl resonances in 2D and 3D experiments for studies of high molecular weight proteins, as

isolated monomers or in complexes. This approach not only unambiguously identifies the residue types, but also resolves overlapped resonances in ^{1}H–^{13}C methyl-correlation spectra. A previously reported experiment aimed to selectively detect the methyl groups of Val and Leu based on the chemical shifts of the carbons directly bonded to the methyl group, i.e., C_β of Val and C_γ of Leu (Van Melckebeke et al. 2004). Since the chemical shifts of C_β of Val and C_γ of Leu are close to each other, the previous method could not reliably distinguish between the two residue types. The significant advance generated by our method arises from the use of the wide separation of chemical shifts between C_α of Val and C_β of Leu. In addition, our 2D experiments allow further selection of the methyl groups of Val or Leu based on their C_α(Val) or C_β(Leu) chemical shifts. In the 3D experiment presented in this study, Val and Leu are clearly separated by the third dimension that encodes the chemical shift of the adjacent carbon and by the opposite signs of the Val and Leu cross peaks. The 3D experiment also allows identification of the methyl pairs within the same residue based on the correlation to the same directly bonded carbon.

We estimated that our method is applicable to proteins or their complexes of at least 360 kDa. The previously developed HMCM[CG]CBCA experiment (Tugarinov and Kay 2003), which correlates H_m, C_m resonances of Val, Leu and Ile to all carbons up to C_α, has a 14 ms longer transverse relaxation period than that used in the 2D V/L-CT-C_mH_m method, not including the real time t_1 labeling period. In addition, there was a reduction in sensitivity (0.5 and 0.25 for Val and Leu residues, respectively) due to the two $4\tau_b$ C–C COSY steps. Because the HMCM[CG]CBCA approach has been successfully used on a 360 kDa subunit of the proteasome (Sprangers and Kay 2007), the experiments presented here should be applicable to proteins of similar or larger sizes.

The experiments presented herein are applicable to protein samples prepared with the widely used protocols using [$^{13}CH_3$, $^{13}CH_3$]-α-ketoisovalerate (Goto et al. 1999), [$^{13}CH_3$, $^{12}CD_3$]-α-ketoisovalerate (Tugarinov and Kay 2003), or 2S ^{1}H,^{13}C-labeled acetolactate (Gans et al. 2010) as precursors to achieve methyl labeling. The experiments also require ^{13}C labeling of the carbons one and two bonds away from the methyl groups, along with ^{2}H labeling. For samples prepared with protonation at one methyl group and deuteration at the other, the method using multiple-quantum coherence during the COSY transfer step (Supplemental Figure S1) should provide improved sensitivity because it fully exploits the methyl-TROSY principle.

The methods presented in this study facilitate methyl-based NMR studies of high molecular weight proteins in several ways. First, these experiments allow the identification of residue types quickly, significantly reducing ambiguity in structure-based assignments of methyl resonances. An added benefit of this approach is to associate the methyl resonances with their C_α or C_β chemical shifts to facilitate resonance assignments based on available crystal structures using the established relationships of C_α and C_β chemical shifts with backbone conformation (Shen and Bax 2010; Xu and Case 2002). For example, for the two sub-spectra obtained with I-BURP pulses at 65.6 and 68.1 ppm, which covers C_α from 64.2 to 69.5 ppm, there are 17 resolved Val residues in MSG, and they are all located in α-helices. Second, because the methods can resolve overlap resonances in 2D spectra, they can be used to increase the number of probes available for studies of protein structure, dynamics, and molecular interactions, and allow assignments of overlapped resonances by site-directed mutagenesis. Overall, the methods presented here will greatly facilitate studies of high molecular weight proteins using the methyl-TROSY approach, particularly in the absence of an ultra-high field NMR spectrometer.

Acknowledgments We thank Dr. Vitali Tugarinov (University of Maryland) for the MSG expression plasmid and Mr. Loren Colson for assistance with protein production. The research was supported by NIH grants R01GM074748 and R01GM086171, an AMMI grant, and the NMR core facility of City of Hope.

References

Delaglio F, Grzesiek S, Vuister GW, Zhu G, Pfeifer J, Bax A (1995) NMRPipe: a multidimensional spectral processing system based on UNIX pipes. J Biomol NMR 6:277–293

Gans P, Hamelin O, Sounier R, Ayala I, Dura MA, Amero CD, Noirclerc-Savoye M, Franzetti B, Plevin MJ, Boisbouvier J (2010) Stereospecific isotopic labeling of methyl groups for NMR spectroscopic studies of high-molecular-weight proteins. Angew Chem Int Ed Engl 49:1958–1962

Gardner KH, Kay LE (1997) Production and incorporation of 15N, 13C, 2H (1H-δ1 methyl) isoleucine into proteins for multidimensional NMR studies. J Am Chem Soc 119:7599–7600

Geen H, Freeman R (1991) Band-selective radiofrequency pulses. J Magn Reson 93:93–141

Gelis I, Bonvin AM, Keramisanou D, Koukaki M, Gouridis G, Karamanou S, Economou A, Kalodimos CG (2007) Structural basis for signal-sequence recognition by the translocase motor SecA as determined by NMR. Cell 131:756–769

Goto NK, Gardner KH, Mueller GA, Willis RC, Kay LE (1999) A robust and cost-effective method for the production of Val, Leu, Ile (delta 1) methyl-protonated 15N-, 13C-, 2H-labeled proteins. J Biomol NMR 13:369–374

Guo C, Tugarinov V (2010) Selective 1H- 13C NMR spectroscopy of methyl groups in residually protonated samples of large proteins. J Biomol NMR 46:127–133

Hu W, Zuiderweg ERP (1996) Stereospecific assignments of Val and Leu methyl groups in a selectively 13C-labeled 18 kDa polypeptide using 3D CT-(H)CCH-COSY and 2D 1Jc-c edited heteronuclear correlation experiments. J Magn Reson B 113:70–75

Janin J, Miller S, Chothia C (1988) Surface, subunit interfaces and interior of oligomeric proteins. J Mol Biol 204:155–164

John M, Schmitz C, Park AY, Dixon NE, Huber T, Otting G (2007) Sequence-specific and stereospecific assignment of methyl groups using paramagnetic lanthanides. J Am Chem Soc 129:13749–13757

Johnson BA, Blevins RA (1994) NMR view: a computer program for the visualization and analysis of NMR data. J Biomol NMR 4:603–614

Kato H, van Ingen H, Zhou BR, Feng H, Bustin M, Kay LE, Bai Y (2011) Architecture of the high mobility group nucleosomal protein 2-nucleosome complex as revealed by methyl-based NMR. Proc Natl Acad Sci U S A 108:12283–12288

Kupce E, Boyd J, Campbell ID (1995) Short selective pulses for biochemical applications. J Magn Reson B 106:300–303

Marino JP, Diener JL, Moore PB, Griesinger C (1997) Multiple-quantum coherence dramatically enhances the sensitivity of CH and CH2 correlations in uniformly C-13-labeled RNA. J Am Chem Soc 119:7361–7366

Marion D, Ikura M, Tschudin R, Bax A (1989) Rapid recording of 2d Nmr-spectra without phase cycling—application to the study of hydrogen-exchange in proteins. J Magn Reson 85:393–399

Marley J, Lu M, Bracken C (2001) A method for efficient isotopic labeling of recombinant proteins. J Biomol NMR 20:71–75

McCaldon P, Argos P (1988) Oligopeptide biases in protein sequences and their use in predicting protein coding regions in nucleotide sequences. Proteins 4:99–122

Pervushin K, Riek R, Wider G, Wuthrich K (1997) Attenuated T2 relaxation by mutual cancellation of dipole–dipole coupling and chemical shift anisotropy indicates an avenue to NMR structures of very large biological macromolecules in solution. Proc Natl Acad Sci U S A 94:12366–12371

Religa TL, Sprangers R, Kay LE (2010) Dynamic regulation of archaeal proteasome gate opening as studied by TROSY NMR. Science 328:98–102

Ruschak AM, Religa TL, Breuer S, Witt S, Kay LE (2010) The proteasome antechamber maintains substrates in an unfolded state. Nature 467:868–871

Shaka AJ, Keeler J, Frenkiel T, Freeman R (1983) An improved sequence for broad-band decoupling—Waltz-16. J Magn Reson 52:335–338

Shen Y, Bax A (2010) SPARTA plus: a modest improvement in empirical NMR chemical shift prediction by means of an artificial neural network. J Biomol NMR 48:13–22

Sheppard D, Guo CY, Tugarinov V (2009) 4D (1)H-(13)C NMR spectroscopy for assignments of alanine methyls in large and complex protein structures. J Am Chem Soc 131:1364–1365

Sprangers R, Kay LE (2007) Quantitative dynamics and binding studies of the 20S proteasome by NMR. Nature 445:618–622

Sprangers R, Li X, Mao X, Rubinstein JL, Schimmer AD, Kay LE (2008) TROSY-based NMR evidence for a novel class of 20S proteasome inhibitors. Biochemistry 47:6727–6734

Tjong H, Qin S, Zhou HX (2007) PI2PE: protein interface/interior prediction engine. Nucleic Acids Res 35:W357–W362

Tugarinov V, Kay LE (2003) Ile, Leu, and Val methyl assignments of the 723-residue malate synthase G using a new labeling strategy and novel NMR methods. J Am Chem Soc 125:13868–13878

Tugarinov V, Kay LE (2004a) An isotope labeling strategy for methyl TROSY spectroscopy. J Biomol NMR 28:165–172

Tugarinov V, Kay LE (2004b) Stereospecific NMR assignments of prochiral methyls, rotameric states and dynamics of valine residues in malate synthase G. J Am Chem Soc 126:9827–9836

Tugarinov V, Muhandiram R, Ayed A, Kay LE (2002) Four-dimensional NMR spectroscopy of a 723-residue protein: chemical shift assignments and secondary structure of malate synthase g. J Am Chem Soc 124:10025–10035

Tugarinov V, Hwang PM, Ollerenshaw JE, Kay LE (2003) Cross-correlated relaxation enhanced 1H[bond]13C NMR spectroscopy of methyl groups in very high molecular weight proteins and protein complexes. J Am Chem Soc 125:10420–10428

Van Melckebeke H, Simorre JP, Brutscher B (2004) Amino acid-type edited NMR experiments for methyl–methyl distance measurement in 13C-labeled proteins. J Am Chem Soc 126:9584–9591

Vuister GW, Bax A (1992) Resolution enhancement and spectral editing of uniformly 13C-enriched proteins by homonuclear broadband 13C decoupling. J Magn Reson 98:428–435

Xu XP, Case DA (2002) Probing multiple effects on 15N, 13C alpha, 13C beta, and 13C′ chemical shifts in peptides using density functional theory. Biopolymers 65:408–423

Xu Y, Liu M, Simpson PJ, Isaacson R, Cota E, Marchant J, Yang D, Zhang X, Freemont P, Matthews S (2009) Automated assignment in selectively methyl-labeled proteins. J Am Chem Soc 131:9480–9481

Zhu G, Bax A (1990) Improved linear prediction for truncated signals of known phase. J Magn Reson 90:405–410